

---

# Training Deep Spiking Neural Networks

---

**Eimantas Ledinauskas   Julius Ruseckas   Alfonsas Juršėnas**  
Baltic Institute of Advanced Technology (BPTI)  
Pilies 16-8, LT-01403, Vilnius, Lithuania  
{eimantas.ledinauskas, julius.ruseckas, alfonsas.jursenas}@bpti.eu

**Giedrius Buračas**  
SRI International, USA  
giedrius.burachas@sri.com

## Abstract

Computation using brain-inspired spiking neural networks (SNNs) with neuromorphic hardware may offer orders of magnitude higher energy efficiency compared to the current analog neural networks (ANNs). Unfortunately, training SNNs with the same number of layers as state of the art ANNs remains a challenge. To our knowledge the only method which is successful in this regard is supervised training of ANN and then converting it to SNN. In this work we directly train deep SNNs using backpropagation with surrogate gradient and find that due to implicitly recurrent nature of feed forward SNN's the exploding or vanishing gradient problem severely hinders their training. We show that this problem can be solved by tuning the surrogate gradient function. We also propose using batch normalization from ANN literature on input currents of SNN neurons. Using these improvements we show that it is possible to train SNN with ResNet50 architecture on CIFAR100 and Imagenette object recognition datasets. The trained SNN falls behind in accuracy compared to analogous ANN but requires several orders of magnitude less inference time steps (as low as 10) to reach good accuracy compared to SNNs obtained by conversion from ANN which require on the order of 1000 time steps.

## 1 Introduction and related work

Spiking neural networks (SNNs) are the brain inspired artificial neural network models that (if implemented in neuromorphic hardware) offer better energy efficiency due to sparse event-driven and asynchronous information processing [30]. It was shown that SNNs computation capacity is theoretically at least not smaller than analog neural networks (ANN's) [20]. There are two important differences of SNNs with respect to analog neural networks (ANN): the activation function is not differentiable and SNNs are inherently recurrent due to accumulation of membrane potential.

Recently it was demonstrated that deep convolutional ANN weights could be transferred to SNN with only a minor loss in visual recognition accuracy [7, 27]. SNNs obtained by conversion are constrained to only use rate encoding and because of that their expressive capacity may be reduced in comparison to SNNs with more complex temporal encoding capabilities. Other drawback of such conversion is that one needs to use on the order of 1000 forward propagation time steps (during inference procedure) for SNN to reach a similar image classification accuracy as ANN counterpart. This drawback severely limits the computation speed and energy efficiency benefit of SNNs. Many inference time steps may be required because the conversion procedure is designed to use rate encoding and large numbers of spikes are required in order to reduce the uncertainty of spiking frequency values. In addition, ANN architectures are constrained [7, 27] (e.g. batchnormalization cannot be used) before the conversion to SNN, this limits ANN performance and upper bound of SNN performance; When using conversion

one can not apply online learning methods, therefore it is unusable for continual learning, real time adaptation. All of mentioned limitations of conversion motivates the search for a way to train SNNs directly instead of only converting ANN parameters to SNN.

Training SNNs remains a difficult task in comparison to training of ANN's. The primary reason for this difficulty is the discontinuous activation function which prevents direct usage of gradient-based optimization. Despite the non-differentiable nature of SNN activations, various workarounds enabling the usage of backpropagation algorithm can be found in the scientific literature.

First approach is to constrain the total number of spikes per neuron during inference [4, 21], the timing of the spikes can be differentiated enabling backpropagation. However, the constraint of certain number of firings per neuron might significantly limit the expressive capacity of the network. Second approach is bio-inspired learning algorithms like spike-timing dependent plasticity for unsupervised learning [15] and reward modulation for supervised learning [2]. Yet these methods remain not effective enough to train deep networks with more than a few layers and even with only a single hidden layer fail to reach the classification accuracy of analogous ANN's trained with backpropagation algorithm. Third approach is to approximate the discontinuous spike activation function as a smooth one during training. This enables using backpropagation algorithm directly with a cost that the network must use different activation functions during training and inference [23]. Fourth approach exploits the observation that the absolute accuracy of the gradients is not necessary for successful training and uses surrogate gradients of spike activation functions in place of the real ones enabling the direct training of true SNNs with backpropagation [23].

One of the first uses of surrogate derivatives have been described in [3]. Different forms of surrogate gradient have been proposed: piece-wise linear  $\beta \max\{0, 1 - |U - \vartheta|\}$  [3, 9, 1], derivative of a fast sigmoid  $[1 + |\gamma(U - \vartheta)|]^{-2}$  [33], exponential function  $\beta \exp\{-\gamma|U - \vartheta|\}$  [28], rectangular  $\beta \text{sign}\{\gamma - |U - \vartheta|\}$  [32]. As the experience shows, the specific functional form of surrogate gradient is not important.

To our knowledge, from all of the training approaches described in the previous paragraphs the methods based on surrogate gradients have achieved the best results. For example, in [32] and [18] the authors managed to almost reach the accuracy of converted SNN's on CIFAR10 with ResNet11 architecture. However, until now, successful training of very deep architectures like ResNet50 has not been demonstrated. Up to this day the best performance on complex datasets like ImageNet or CIFAR100 with deep SNN architectures (e.g. ResNet50) has been achieved by supervised training ANN and then converting it to SNN [27, 18].

In this article we explore the possibility to directly train very deep SNNs. To achieve that we use surrogate gradients as proposed in [23]. We found that with increasing number of neuron layers the exploding or vanishing gradients quickly become a problem severely hindering the training. This might be explained by the fact that SNN could be understood as an RNN due to accumulation of membrane potential of a neuron (see figure 1). When backpropagation algorithm is used, SNN inherits vanishing and exploding gradient problems of RNN's due to a deep unrolled computational graph. We found that this problem can be solved by tuning the surrogate gradient function. We also propose using batch normalization on the input currents of the neurons. These simple improvements let us directly train very deep SNNs (e.g. ResNet50) on complex datasets like CIFAR100 [16] or Imagenette [13]. To our knowledge, such deep SNNs have never been directly trained successfully before and could only be obtained by conversion from ANN. By training SNNs directly we are unable to reach the accuracy of analogous ANN's, but we find that our networks require orders of magnitude less inference time steps (as low as 10) to already reach good performance. This might be very important in order to minimize the inference time and energy costs in the real world applications.

## 2 Methods

### 2.1 Architecture of spiking neural networks

In this work we focus on computer vision domain and specifically on image recognition. We take common architectures of convolutional neural networks and replace the nonlinearities by spiking neurons. As is suggested in [25], the analog input image is encoded into a spike train at the first hidden layer by injecting a constant input current into a spiking neuron. At the output of the network analog current from the neurons of the last layer are summed (as in a spiking neuron with very large

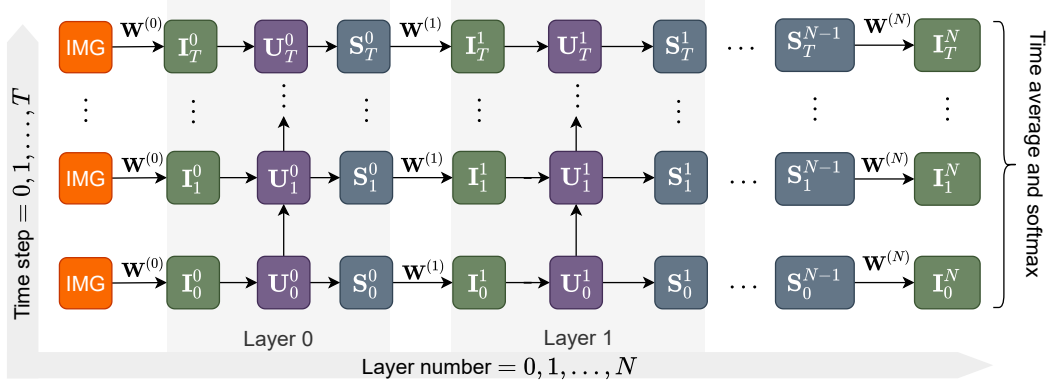


Figure 1: SNN diagram unrolled in time, here  $\mathbf{W}^{(n)}$  denotes the weight matrix,  $\mathbf{I}_t^n$  - electric currents,  $\mathbf{U}_t^n$  - synaptic potentials,  $\mathbf{S}_t^n$  - spikes, for layer  $n$  and time step  $t$ .

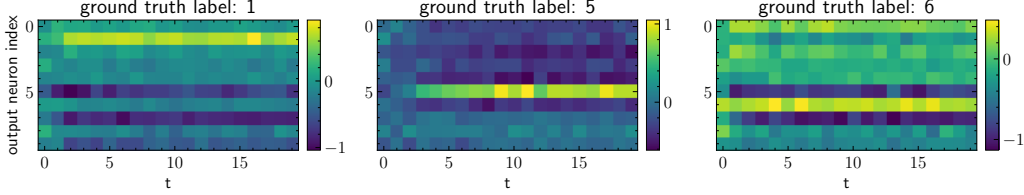


Figure 2: Examples of output currents (in arbitrary units) from the last layer neurons of the network trained on CIFAR10 dataset. Vertical axis denotes the output neuron index and horizontal axis denotes time step number. Ground truth labels of the given examples are written above the images.

threshold) and treated as class logits [25, 18]. For numerical simulation we discretize time. In this way SNNs constitute a special case of RNNs with the time-unrolled computational graph shown in figure 1. The typical output of the last layer of an SNN is shown in figure 2.

## 2.2 Integrate and fire neuron model

In order to minimize the number of possible hyperparameters, in this article we use a simple integrate and fire (IF) neuron model. Such a model is sufficient for time-independent classification tasks. For more complicated, time-dependent tasks more complex neuron models, at least leaky integrate and fire (LIF), might be needed.

The dynamics of the membrane potential  $U(t)$  of IF neuron are described by the equations [10]

$$C \frac{d}{dt} U_j(t) = I_j(t), \quad I_j(t) = \sum_i W_{ji} S_i(t), \quad (1)$$

where  $C$  is membrane capacitance and  $I_j(t)$  is the input synaptic current. The input current is a weighted sum of pre-neuron spikes  $S_i(t)$ , with the connecting weights being  $W_{ji}$ . When the membrane potential  $U$  reaches the threshold value  $\vartheta$ , the neuron generates an output spike and the membrane potential  $U$  is reduced to the rest potential  $U_{\text{rest}}$ . We modify equation (1) to be evaluated in discrete time steps replacing the differential equation by the difference equation:

$$u_j^t = u_j^{t-1} + \sum_i w_{ji} s_i^{t-1}. \quad (2)$$

The output spike is  $s_j^t = 1$  if  $u_j^{t-1} > \vartheta$  and  $s_j^t = 0$  otherwise. Once the spike  $s_j^t$  is generated, the membrane potential is reset. In this article we consider two types of reset: reset to zero  $u_j^{t+1} = u_j^t (1 - s_j^t)$  (hard reset) [7] and reset by subtraction  $u_j^{t+1} = u_j^t - \vartheta s_j^t$  (soft reset) [5, 8]. It has been

argued [25, 11] that soft reset reduces the information loss and improves ANN-SNN conversion. We found that training shallow (several layers) models with soft reset allows us to obtain better classification accuracy, compared to models with hard reset. However in deep models hard reset performs better. We hypothesize that the advantage of hard reset for deeper models might be related to the accumulation of inaccuracies due to surrogate gradient (see section 4) because after a hard reset the time history of the membrane potential is forgotten.

### 2.3 Surrogate gradient for training a single neuron

Let us consider at first a single neuron and investigate how to train the neuron for emitting a given spike train  $S_{\text{gt}}(t)$  for a given stimulus. Employing a physical analogy we propose to use as a loss function the energy of the error that we define as follows: the energy is a time integral of power which is equal to the error current  $S_{\text{err}}(t) = S(t) - S_{\text{gt}}(t)$  multiplied by the membrane potential  $U(t)$ . Thus we consider the loss

$$\mathcal{L} = \int_0^T S_{\text{err}}(t)U(t) dt = \int_0^T (S(t) - S_{\text{gt}}(t))U(t) dt \quad (3)$$

Here  $T$  is the total duration of the spike train. Such a loss does not have a problem with the non-differentiability of the spiking nonlinearity because the gradient of the output  $S(t)$  is zero almost everywhere and can be neglected. The gradient of this loss is similar to the gradient in SuperSpike [33], with the function  $\sigma(U) = U$ . One can see that the loss (3) has some desirable properties: the loss decreases with increasing membrane potential when the output pulse is missing ( $S - S_{\text{gt}} < 0$ ) thus causing the appearance of the output pulse. If the output pulse should not be present ( $S - S_{\text{gt}} > 0$ ), the loss decreases with decreasing membrane potential. The drawback of such a loss is that it can acquire both positive and negative values, and values close to zero can be obtained when membrane potential is close to zero even if output pulses differ from the desired ones. However, the optimal values of the weights still correspond to the gradient of the loss being zero.

In analogy with the van Rossum distance we can define a more general loss

$$\mathcal{L} = \int_0^T [(\alpha * S)(t) - (\alpha * S_{\text{gt}})(t)](\alpha * U)(t) dt, \quad (4)$$

where

$$(\alpha * X)(t) \equiv \int_0^t \alpha(t - t')X(t') dt' \quad (5)$$

denotes a convolution. A single neuron can be used also in classification tasks, for example to determine if the number of pulses is larger than a given threshold. In analogy with equation (3), we take the convolution kernel  $\alpha(t) = 1$  for whole duration  $T$  and propose the following loss for classification tasks:

$$\mathcal{L} = [\Theta(Y) - Y_{\text{gt}}] \int_0^T U(t) dt, \quad Y = \int_0^T S(t) dt. \quad (6)$$

Here  $\Theta$  is a Heaviside step function,  $Y_{\text{gt}} = 0, 1$  is a ground-truth label.

The gradient of the loss function (3) can be obtained in the following way: we can consider the functions

$$\mathcal{L}' = \frac{1}{2} \int_0^T [S(t) - S_{\text{gt}}(t)]^2 dt$$

instead of (3) and

$$\mathcal{L}' = \frac{1}{2} [\Theta(Y) - Y_{\text{gt}}]^2$$

instead of (6) together with a replacement rule

$$\nabla S \rightarrow \nabla U. \quad (7)$$

That is, the gradient of a non-differentiable spike is replaced by another, surrogate, gradient [23].

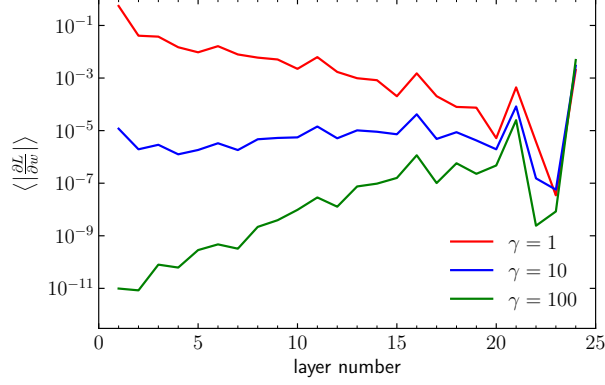


Figure 3: Average magnitude of loss gradient dependence on layer number with different values of surrogate gradient parameter  $\gamma$ . Gradient explodes if  $\gamma$  is too small and vanishes if it is too large. ResNet18 architecture was used in this picture.

## 2.4 Surrogate gradient for multi-layer spiking neural network

A way of training SNN with backpropagation is to replace the gradient of a non-differentiable spike by another, surrogate, gradient [23]. The simplest replacement is just  $\nabla S \rightarrow \nabla U$ . However, such simple surrogate gradient causes problems when applied to multi-layer spiking neural network. In the situation when the potential of a neuron in a hidden layer is close to zero, the application of gradient descent with the surrogate gradient causes the potential to increase or decrease with almost equal probabilities, and the potential remains close to zero for a long time. In order to avoid this, we modify the replacement rule as

$$\nabla S \rightarrow f(U)\nabla U, \quad (8)$$

with function  $f(U)$  being smaller when the potential is close to zero:  $f(0) < f(\vartheta)$ . Numerical experiments show, that the actual form of the function  $f(U)$  is not important. In this article we take

$$f(U) = \beta\{1 + [\gamma(U - \vartheta)]\}^{-2}. \quad (9)$$

Here  $\beta$  (we use  $\beta = 1$ ) is a hyper-parameter determining the size of the surrogate gradient and  $\gamma$  determines the width of the gradient. As the discussion above shows, the value  $\gamma = 0$  is not suitable for deeper SNNs. On the other hand, very large values of  $\gamma$  cause the surrogate gradient to be almost always very small, except in the rare situations when the potential  $U$  is close to the threshold  $\vartheta$ . Thus one should expect that there exist an optimal, intermediate value of  $\gamma$ .

Note, that in spiking neurons with hard reset we take the gradient of spikes  $s_j^t$  to be zero. In this way the previous values of the membrane potential  $u_j$  do not influence the gradient of the potential after the reset, the history of the potential is forgotten after reset.

## 2.5 Tuning of surrogate gradient

Using a surrogate gradient, the gradient of the loss with respect to the membrane potential  $u_l$  in the neuron of  $l$ -th layer is

$$\delta u_l = f(u_l)\delta s_l \quad (10)$$

where  $\delta s_l$  is the gradient of the loss with respect to the output spikes of the  $l$ -th layer. Similarly as in [12], we assume that the elements of the gradient  $\delta s_l$  are mutually independent and share the same distribution. In addition, we assume that  $\delta s_l$  and  $u_l$  are independent of each other and the gradients have zero means,  $\langle \delta u_l \rangle = 0$  and  $\langle \delta s_l \rangle = 0$ . In this case the variances of the gradients obey

$$\text{var}[\delta u_l] = \langle f(u_l)^2 \rangle \text{var}[\delta s_l]. \quad (11)$$

If the probability distribution function of  $u$  is  $P(u)$  with the width  $\sigma_u$  then

$$\langle f(u)^2 \rangle = \int_{-\infty}^{+\infty} f(u)^2 P(u) du \sim \frac{\beta}{\gamma \sigma_u}. \quad (12)$$

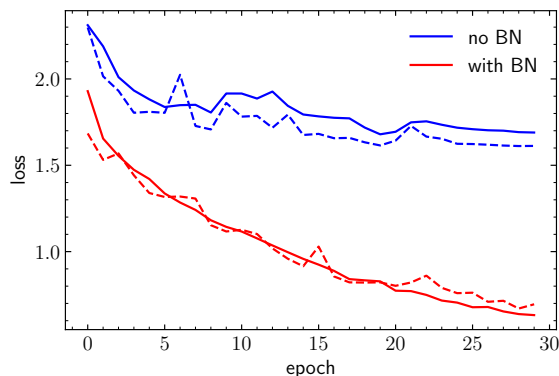


Figure 4: Comparison of typical learning curves for ResNet18 SNN on CIFAR10 dataset trained with (red) and without (blue) batch normalization. The solid and dashed lines denote the training and validation losses respectively.

Furthermore, from equation (2) it follows that the gradient of the loss with respect to the output spikes of the  $l - 1$ -th layer  $\delta s_{l-1}$  is related to the gradient of the potential of the  $l$ -th layer  $\delta u_l$ . The variance of the gradient  $\delta s_{l-1}$  is proportional to

$$\text{var}[\delta s_{l-1}] \sim \text{var}[w_l] \text{var}[\delta u_l] \sim \text{var}[w_l] \langle f(u_l)^2 \rangle \text{var}[\delta s_l]. \quad (13)$$

We see that during the backpropagation the variance of the gradient is multiplied by  $\langle f(u)^2 \rangle$  for each layer. Depending on the value of  $\langle f(u)^2 \rangle$  this can cause exploding or vanishing gradients in the deeper neural networks. To avoid this problem we propose to fine-tune the value of  $\langle f(u)^2 \rangle$ . This can be achieved in three ways: i) by changing the height of the surrogate gradient  $\beta$ , ii) by changing the width of the surrogate gradient  $\gamma$ , iii) by changing the initialization of the model parameters and thus the resulting probability distribution function of the neuron potential. In this article we concentrate our attention on the fine-tuning of the value of the parameter  $\gamma$ .

An example of the behavior of the gradient for different values of  $\gamma$  is shown in figure 3. Here we used SNN with ResNet18 architecture. One can see that for small values of  $\gamma = 1$  the gradient explodes, whereas for large values  $\gamma = 100$  the gradient vanishes. Because of this monotonic relation the optimal  $\gamma$  can be found fast by using bisection search.

## 2.6 Batch normalization for SNNs

Batch normalization layer [14] is a widely used architectural element in ANN literature. It stabilizes the distribution of inputs to a certain network layer by setting their mean and variance to some learnable values. This makes the training of a neural network less sensitive to hyperparameters and to some extent prevents exploding or vanishing gradients [14]. As was shown in [26], batch normalization also increases the smoothness of the loss landscape and thus results in more predictive and well-behaved gradients.

For recurrent neural networks batch normalization has been applied both to the connections from layer to layer [17] and to the recurrent ones [6]. Similarly to [17], in this work we apply batch normalization in SNNs on the input currents to every neuron layer (horizontal connections in figure 1). In effect, this allows for the spiking neurons to learn their firing threshold during training as scaling the input currents is equivalent to changing the threshold. Also this allows for non-zero bias currents which, depending on the sign of their value, are equivalent to the leaking or passive accumulation of the potential. We find that similarly to ANN's the batch normalization in SNNs improves the rate of convergence and decreases the sensitivity to the hyperparameters.

The examples of typical learning curves for ResNet18 SNN's with and without batch normalization can be seen in figure 4. Clearly the training converges much faster with batch normalization. We noticed that this disparity increases even more with increasing network depth. Here in both cases the networks were trained with ADAMW optimizer [19] and fixed learning rate  $5 \cdot 10^{-4}$ . The network

Table 1: State of the art SNN accuracies on MNIST dataset. STDP stands for "Spike-Timing-Dependent-Plasticity".

Model	Method	MNIST accuracy
Mozafari et al. [22]	reward-modulated STDP	97.2
Tavanaei et al. [31]	STDP + gradient descent	98.6
Lee et al. [18]	backpropagation	99.59
<b>This work</b>	<b>backpropagation</b>	<b>99.40</b>

Table 2: State of the art SNN accuracies on CIFAR10 dataset.

Model	Method	CIFAR10 accuracy
Wu et al. [32]	backpropagation	90.53
Lee et al. [18]	backpropagation	90.95
Han et al. [11]	ANN-SNN conversion	93.63
Rathi et al. [24]	ANN-SNN conversion	92.94
<b>This work</b>	<b>backpropagation</b>	<b>90.20</b>

without batch normalization additionally requires initial normalization of spiking thresholds because otherwise the spiking activity of the neurons could be too low or too high. In both cases the training is very slow and might not even happen at all. To normalize the thresholds we follow the method used in ANN to SNN conversion [27] and set the threshold of the neuron layer to the maximum value of the input current to this layer throughout the whole training dataset and all time steps.

### 3 Results

#### 3.1 Training methodology

In this section we describe the general details about training which apply to all of the models presented in this paper unless stated otherwise.

For optimization we used ADAMW [19] algorithm with weight decay parameter 0.01. The learning rate was changed according to one-cycle learning rate schedule [29]. The maximum learning rates for the schedule were chosen by using learning rate range test as proposed in [29] for every network separately. We also used batchnormalization layers between convolution (or fully-connected) and activation layers for both ANNs and SNNs (see section 2.6). During SNN training we use 10 time steps for their simulation (justification for this can be found in 3.4). Also for SNNs we fine-tune gamma so that the average magnitude of the gradient of the layers in the first half of the network would be as close as possible to the second half (see 2.5). In the cases of CIFAR10 and CIFAR100 we used random horizontal flip, random crop and color jitter augmentations and in the case of MNIST we did not use any.

#### 3.2 Performance comparison with the other works

In this section we compare the performance achieved by using our method to the state of the art results found in the literature. Table 1 shows the comparison of classification accuracy on hand written digit dataset MNIST. Table 2 shows the comparison of classification accuracy on object recognition dataset CIFAR10.

For MNIST dataset we have used a simple convolutional SNN consisting of two convolutional layers (32 and 64 channels,  $5 \times 5$  kernels) that are followed by  $2 \times 2$  average pooling. After the convolutional part there are two fully connected layers, the first of which has size 1024. We use dropout with probability 0.5 before the last layer. Note, that for such a shallow network we did not employ batch normalization and used spiking neurons with soft reset. For evaluation 20 time steps were used. The achieved accuracy is shown in table 1.

For CIFAR10 dataset we used ResNet11 SNN, similar as in [18] but with added batch normalization. For evaluation 20 time steps were used. The achieved accuracy is shown in table 2.

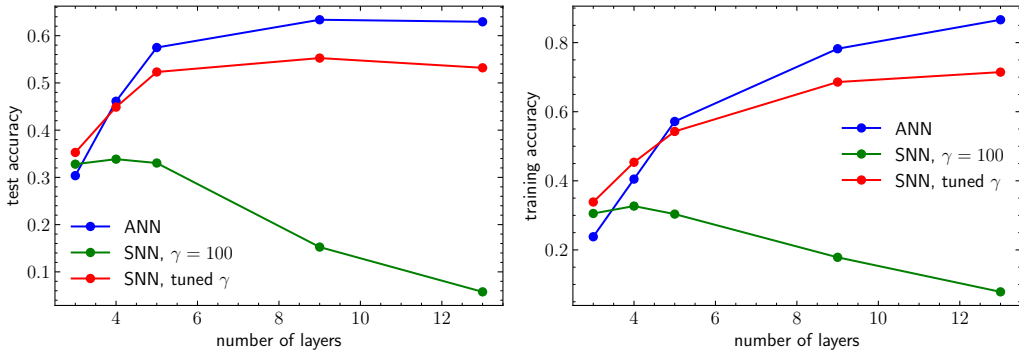


Figure 5: The dependence of final test (left) and training (right) accuracies on the number of layers in the network for ANN (blue), SNN with fixed  $\gamma = 100$  (green) and SNN with fine-tuned gamma (red).

Table 3: CIFAR100 accuracy comparison between our ResNet50 SNN and networks obtained by ANN-SNN conversion.

Model	Method	CIFAR100 accuracy
Han et al. [11]	VGG16, ANN-SNN conversion	70.93
Rathi et al. [24]	VGG11, ANN-SNN conversion	70.94
<b>This work</b>	<b>Resnet50, backpropagation</b>	<b>58.5</b>

### 3.3 Scaling up to deeper SNN's

In order to determine how training of SNN's with surrogate gradient scales with number of layers in the network we have trained 5 simple convolutional classifier architectures with 3, 4, 5, 9 and 13 layers. The first three networks have 2, 3 and 4 convolutional layers with stride = 2. The last two networks have 4 blocks with 2 and 3 convolutional layers repeated of which only the first in the block has stride = 2. The number of channels after the first convolution is 32 and is subsequently doubled after every layer with stride = 2. In all of the networks after all of the convolutional layers there is the last single fully-connected layer mapping the last feature map to the class confidence scores. We trained these networks on CIFAR100 object recognition dataset. For every architecture we trained 3 variants: ANN, SNN with a fixed  $\gamma = 100$  (see eq. 9, the value was taken from associated code of [23]) and SNN with fine-tuned gamma. For ANN variants the ReLU activation was used after every convolutional layer and for SNN's the simple integrate and fire neurons were used as described in section 2.2.

The main results of this experiment can be seen in fig. 5 where the dependencies of the final testing and training accuracies on number of layers in these networks are shown. It is clear that without fine-tuned  $\gamma$  only shallow networks can be effectively trained as already at 5 layers both testing and training accuracies are starting to decline with increasing number of layers.

It is interesting that with 3 and 4 layers SNNs achieve higher test accuracy than analogous ANNs (although higher test accuracy is achieved only with 3 layers). This is evidence that SNNs might have higher expressive capacity than ANNs due to complex time encoding capabilities. However with increasing number of layers the ANN accuracy grows more quickly and already at 5 layers overcomes the SNN accuracy. The worse scaling of SNN performance might be explained by the fact that the surrogate gradient inaccuracy grows larger with increasing number of layers as described in more detail in section 4.

To demonstrate training on more complex datasets with very deep network we also trained ResNet50 SNN on CIFAR100 and a subset of ImageNet [13]. In the latter case we used images rescaled to  $128 \times 128$  pixels. For evaluation 40 and 20 time steps were used respectively. The model achieved 81.2% accuracy on ImageNet subset and 58.5 % on CIFAR100. The result of training on CIFAR100 is shown in table 2



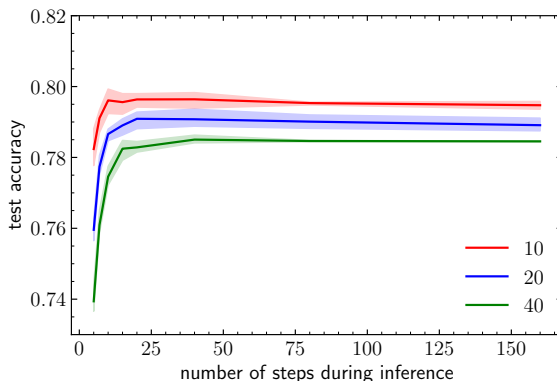


Figure 6: Test accuracy dependence on number of time steps during inference for three different numbers of time steps during training: 10 (red), 20 (blue) and 40 (green). The lines denote the average between the networks with different random initializations. The colored areas around the lines denote the intervals between minimum and maximum values.

### 3.4 Accuracy dependence on inference time steps

To investigate how our SNN performance varies with different number of time steps used to simulate the network we trained a small SNN using 10, 20 and 40 time steps. We used the architecture from section 3.3 with 4 convolutional layers. To estimate the stochasticity we trained networks with 3 different random parameter initializations in every case. After training the evaluation can be done with increased or decreased number of time steps. How this changes the networks accuracy in cases when it was trained with 10, 20 and 40 time steps can be seen in fig. 6. Interestingly, we can see that increasing SNN time steps during inference beyond the number that it was trained with does not improve the accuracy. This behavior of our SNNs is very different compared to SNNs obtained by conversion from ANNs where increasing the number of time steps does increase the accuracy and 1000-2000 steps are needed to reach the accuracy close to the original ANN. This difference most probably arises because our SNNs learn to exploit more expressive time encoding in order to make predictions in short time instead of a more inefficient rate encoding used in converted SNNs. The other surprising trend that can be seen in figure 6 is that the maximum accuracy decreases with increasing number of time steps during training. This might be related to the problematic SNN scaling demonstrated in section 3.3 because the increase of the number of time steps is similar to the increase of the network depth when using backpropagation through time (the unrolled computational graph gets deeper).

## 4 Discussion and Conclusions

In this work we showed that it is possible to train deep SNNs with minimal methodological changes compared to ANNs. Moreover, the described method is simple to implement with popular deep learning frameworks designed primarily for ANNs by just implementing a custom gradient function for the spiking activation and then fine-tuning  $\gamma$  as described in section 2.5. This makes it easy to benefit from the vast contemporary deep learning infrastructure when working with SNNs. Also, by using existing deep learning frameworks it is possible to create architectures incorporating both ANNs and SNNs into a single network which can be trained end-to-end. This might prove useful in some applications as SNNs might have advantages in some tasks compared to ANNs and vice versa.

The biggest shortcoming of our method is that with increasing number of layers in the network eventually the performance starts to decrease and this prevents the usage of the deepest architectures used in the literature. Our hypothesis is that the difference between the effective loss that is minimized by surrogate gradient and the loss that we actually want to minimize grows with increasing number of layers or simulated time steps. We plan to study this issue in more detail in the future. Still we think that the identification and solution of exploding and vanishing gradient problem that we presented here is a significant step forward towards training SNNs of any depth.

Another issue that we think is worthwhile to investigate in the future is that effective training of SNNs may require significantly different architectures in comparison to ANNs. In this work we have used only architectures that were developed for ANNs. This might at least partially explain why it is so hard to reach ANN performance with SNNs while training models from scratch.

In summary, the main conclusions of this work are the following: **i)** exploding and vanishing problems in deep SNNs can be solved by tuning surrogate gradient width parameter  $\gamma$ ; **ii)** batch normalization of the neuron input currents helps training SNNs similarly like batch normalization in ANNs; **iii)** several orders of magnitude less inference time steps are needed when training SNNs from scratch (in comparison to SNNs converted from ANNs); **iv)** with shallow architectures SNNs can sometimes achieve better performance than analogous ANNs. This might be important in autonomous IoT and Edge devices; **v)** the performance of SNNs trained with surrogate gradients grows slower than that of ANNs with increasing layers and even starts to diminish at some point even if the gradients do not explode or vanish.

## Broader Impact

Currently SNNs still lag behind ANNs in terms of their accuracy on a wide variety of deep learning tasks. The greatest obstacle for bridging this gap is training deeper SNNs, and to date training networks deeper than a few layers remained a challenge. ANN-to-SNN conversion methods, on the other hand require a separate ANN pretraining step on GPUs and thus are not compatible with on-device, on-line learning. Thus, effective training methods for SNNs could enable a wider adoption of energy-efficient neuromorphic hardware in autonomous, IoT and Edge devices. Also, this kind of hardware might be especially relevant for applications in space (e.g. nanosatellites).

While our results are promising in terms of supervised training of deep SNNs approaching that of ANNs, a number of questions remain to be investigated. A negative outcome of our research would potentially signal a failure of SNNs to match ANN learning capabilities, and so could result in limited applicability of deep learning advances for neuromorphic technology.

From ethical standpoint we do not see any special consequences apart from those associated with general technological progress.

## References

- [1] G. Bellec, D. Salaj, A. Subramoney, R. Legenstein, and W. Maass. Long short-term memory and learning-to-learn in networks of spiking neurons. In S. Bengio, H. Wallach, H. Larochelle, K. Grauman, N. Cesa-Bianchi, and R. Garnett, editors, *Advances in Neural Information Processing Systems 31*, pages 787–797. Curran Associates, Inc., 2018.
- [2] Zhenshan Bing, Ivan Baumann, Zhuangyi Jiang, Kai Huang, Caixia Cai, and Alois C Knoll. Supervised learning in snn via reward-modulated spike-timing-dependent plasticity for a target reaching vehicle. *Frontiers in neurorobotics*, 13:18, 2019.
- [3] S. M. Bohte. Error-backpropagation in networks of fractionally predictive spiking neurons. In T. Honkela, W. Duch, M. Girolami, and S. Kaski, editors, *Artificial Neural Networks and Machine Learning – ICANN 2011*, volume 6791 of *Lecture Notes in Computer Science*, pages 60–68, Berlin, Heidelberg, 2011. Springer.
- [4] Sander M Bohte, Joost N Kok, and Han La Poutre. Error-backpropagation in temporally encoded networks of spiking neurons. *Neurocomputing*, 48(1-4):17–37, 2002.
- [5] A. S. Cassidy, P. Merolla, J. V. Arthur, S. K. Esser, B. Jackson, R. Alvarez-Icaza, P. Datta, J. Sawada, T. M. Wong, V. Feldman, A. Amir, D. B. Rubin, F. Akopyan, E. McQuinn, W. P. Risk, and D. S. Modha. Cognitive computing building block: A versatile and efficient digital neuron model for neurosynaptic cores. In *The 2013 International Joint Conference on Neural Networks (IJCNN)*, pages 1–10, 2013.
- [6] Tim Coijmans, Nicolas Ballas, César Laurent, and Aaron C. Courville. Recurrent batch normalization. *CoRR*, abs/1603.09025, 2016. URL <http://arxiv.org/abs/1603.09025>.

- [7] P. U. Diehl, D. Neil, J. Binas, M. Cook, S. Liu, and M. Pfeiffer. Fast-classifying, high-accuracy spiking deep networks through weight and threshold balancing. In *2015 International Joint Conference on Neural Networks (IJCNN)*, pages 1–8, 2015.
- [8] P. U. Diehl, B. U. Pedroni, A. Cassidy, P. Merolla, E. Neftci, and G. Zarrella. TrueHappiness: Neuromorphic emotion recognition on TrueNorth. In *2016 International Joint Conference on Neural Networks (IJCNN)*, pages 4278–4285, 2016.
- [9] S. K. Esser, P. A. Merolla, J. V. Arthur, A. S. Cassidy, R. Appuswamy, A. Andreopoulos, D. J. Berg, J. L. McKinstry, T. Melano, D. R. Barch, C. di Nolfo, P. Datta, A. Amir, B. Taba, M. D. Flickner, and D. S. Modha. Convolutional networks for fast, energy-efficient neuromorphic computing. *Proc. Natl. Acad. Sci. USA*, 113(41):11441–11446, 2016.
- [10] W. Gerstner, W. M. Kistler, R. Naud, and L. Paninski. *Neuronal dynamics: From single neurons to networks and models of cognition*. Cambridge University Press, 2014.
- [11] B. Han, G. Srinivasan, and K. Roy. RMP-SNN: Residual membrane potential neuron for enabling deeper high-accuracy and low-latency spiking neural network. arXiv:2003.01811, 2020.
- [12] K. He, X. Zhang, S. Ren, and J. Sun. Delving deep into rectifiers: Surpassing human-level performance on imagenet classification. In *2015 IEEE International Conference on Computer Vision (ICCV)*, pages 1026–1034, Santiago, 2015.
- [13] Jeremy Howard. imagenette, 2019. URL <https://github.com/fastai/imagenette/>.
- [14] Sergey Ioffe and Christian Szegedy. Batch normalization: Accelerating deep network training by reducing internal covariate shift. *arXiv preprint arXiv:1502.03167*, 2015.
- [15] Saeed Reza Kheradpisheh, Mohammad Ganjtabesh, Simon J Thorpe, and Timothée Masquelier. Stdp-based spiking deep convolutional neural networks for object recognition. *Neural Networks*, 99:56–67, 2018.
- [16] A. Krizhevsky. Learning multiple layers of features from tiny images. techreport TR-2009, University of Toronto, Toronto, 2009.
- [17] C. Laurent, G. Pereyra, P. Brakel, Y. Zhang, and Y. Bengio. Batch normalized recurrent neural networks. In *2016 IEEE International Conference on Acoustics, Speech and Signal Processing (ICASSP)*, pages 2657–2661, 2016.
- [18] Chankyu Lee, Syed Shakib Sarwar, Priyadarshini Panda, Gopalakrishnan Srinivasan, and Kaushik Roy. Enabling spike-based backpropagation for training deep neural network architectures. *Frontiers in Neuroscience*, 14:119, 2020. ISSN 1662-453X. doi: 10.3389/fnins.2020.00119. URL <https://www.frontiersin.org/article/10.3389/fnins.2020.00119>.
- [19] Ilya Loshchilov and Frank Hutter. Decoupled weight decay regularization. In *International Conference on Learning Representations*, 2019. URL <https://openreview.net/forum?id=Bkg6RiCqY7>.
- [20] Wolfgang Maass and Henry Markram. On the computational power of circuits of spiking neurons. *Journal of computer and system sciences*, 69(4):593–616, 2004.
- [21] Hesham Mostafa. Supervised learning based on temporal coding in spiking neural networks. *IEEE transactions on neural networks and learning systems*, 29(7):3227–3235, 2017.
- [22] Milad Mozafari, Mohammad Ganjtabesh, Abbas Nowzari-Dalini, Simon J. Thorpe, and Timothée Masquelier. Bio-inspired digit recognition using reward-modulated spike-timing-dependent plasticity in deep convolutional networks. *Pattern Recognition*, 94:87–95, 2019.
- [23] E. O. Neftci, H. Mostafa, and F. Zenke. Surrogate gradient learning in spiking neural networks: Bringing the power of gradient-based optimization to spiking neural networks. *IEEE Signal Processing Magazine*, 36(6):51–63, 2019.

- [24] Nitin Rathi, Gopalakrishnan Srinivasan, Priyadarshini Panda, and Kaushik Roy. Enabling deep spiking neural networks with hybrid conversion and spike timing dependent backpropagation. In *International Conference on Learning Representations*, 2020. URL <https://openreview.net/forum?id=B1xSperKvH>.
- [25] B. Rueckauer, I.-A. Lungu, Y. Hu, M. Pfeiffer, and S.-C. Liu. Conversion of continuous-valued deep networks to efficient event-driven networks for image classification. *Front. Neurosci.*, 11: 682, 2017.
- [26] Shibani Santurkar, Dimitris Tsipras, Andrew Ilyas, and Aleksander Madry. How does batch normalization help optimization? In *Advances in Neural Information Processing Systems*, pages 2483–2493, 2018.
- [27] Abhronil Sengupta, Yuting Ye, Robert Wang, Chiao Liu, and Kaushik Roy. Going deeper in spiking neural networks: VGG and residual architectures. *Front. Neurosci.*, 13:95, 2019.
- [28] S. B. Shrestha and G. Orchard. SLAYER: Spike layer error reassignment in time. In S. Bengio, H. Wallach, H. Larochelle, K. Grauman, N. Cesa-Bianchi, and R. Garnett, editors, *Advances in Neural Information Processing Systems 31*, pages 1412–1421. Curran Associates, Inc., 2018.
- [29] Leslie N Smith. A disciplined approach to neural network hyper-parameters: Part 1—learning rate, batch size, momentum, and weight decay. *arXiv preprint arXiv:1803.09820*, 2018.
- [30] Martino Sorbaro, Qian Liu, Massimo Bortone, and Sadique Sheik. Optimizing the energy consumption of spiking neural networks for neuromorphic applications. *arXiv preprint arXiv:1912.01268*, 2019.
- [31] A. Tavanaei, Z. Kirby, and A. S. Maida. Training spiking convnets by stdp and gradient descent. In *2018 International Joint Conference on Neural Networks (IJCNN)*, pages 1–8, 2018.
- [32] Y. Wu, L. Deng, G. Li, J. Zhu, Y. Xie, and L. Shi. Direct training for spiking neural networks: Faster, larger, better. In *The Thirty-Third AAAI Conference on Artificial Intelligence (AAAI-19)*, volume 33, pages 1311–1318. AAAI Press, 2019.
- [33] F. Zenke and S. Ganguli. SuperSpike: Supervised learning in multilayer spiking neural networks. *Neural Computation*, 30(6):1514–1541, 2018.